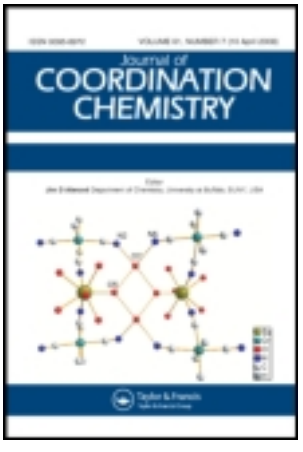

Journal of Coordination Chemistry
Publication details, including instructions for authors and subscription information:
http://www.tandfonline.com/loi/gcoo20

Synthesis and characterization of some potential antitumor palladium(II) complexes of 2-aminomethylbenzimidazole and amino acids

Ahmed A. El-Sherif [a]
[a] Faculty of Science, Department of Chemistry , Cairo University , Giza, Egypt
Published online: 09 Jun 2011.

To cite this article: Ahmed A. El-Sherif (2011) Synthesis and characterization of some potential antitumor palladium(II) complexes of 2-aminomethylbenzimidazole and amino acids, Journal of Coordination Chemistry, 64:12, 2035-2055, DOI: 10.1080/00958972.2011.587004

To link to this article: http://dx.doi.org/10.1080/00958972.2011.587004

Journal of Coordination Chemistry
Vol. 64, No. 12, 20 June 2011, 2035–2055

Synthesis and characterization of some potential antitumor palladium(II) complexes of 2-aminomethylbenzimidazole and amino acids

AHMED A. EL-SHERIF*

Faculty of Science, Department of Chemistry, Cairo University, Giza, Egypt

(*Received 20 January 2011; in final form 12 April 2011*)

The stoichiometry and stability constants of complexes formed between $[Pd(AMBI)(H_2O)_2]^{2+}$ (AMBI = 2-(aminomethyl)-benzimidazole) with some selected bio-relevant ligands containing different functional groups were investigated at 25°C and 0.1 mol L^{-1} ionic strength. The ligands used are imidazole, cysteine, glutathione (GSH), threonine, aspartic acid, 1,1-cyclobutane dicarboxylic acid (CBDCA) and lysine. The stoichiometry and stability constants of the formed complexes were reported and the concentration distribution of the various complex species was evaluated as a function of pH. The results show ring opening of CBDCA and monodentate complexation of the DNA constituent with the formation of [Pd(AMBI)(CBDCA–O)DNA], where (CBDCA–O) represents cyclobutane dicarboxylate coordinated by one carboxylate oxygen. The equilibrium constant of the displacement reaction of coordinated inosine, as a typical DNA constituent, by glutathione, as a typical thiol ligand, was investigated. The effect of dioxane on the formation constant of CBDCA with $Pd(AMBI)^{2+}$ is reported. Five new palladium(II) complexes of the formula $[Pd(AMBI)(AA)]^{n+}$ (where AMBI = 2-aminomethyl benzimidazole, AA is an anion of glycine, alanine, cysteine, methionine, and serine) have been synthesized. These palladium(II) complexes have been ascertained by elemental, molar conductance, infrared and ^{1}H-NMR spectroscopy. The isolated Pd(II) complexes were screened for their antibacterial and cytotoxic activities and the results are discussed.

Keywords: 2-(Aminomethyl)-benzimidazole; Glutathione; DNA; Biological activity; Equilibrium studies; Potentiometric titration

1. Introduction

Cisplatin, *cis*-diamminedichloroplatinum(II), is one of the most effective anticancer agents [1]. It has demonstrated a remarkable chemotherapeutic potential in a large variety of human solid cancers, such as testicular, ovarian, bladder, lung, and stomach carcinomas [2, 3]. The use of platinum(II) complexes as potent anticancer drugs has attracted much interest. The nature and arrangement of the ligands can affect the mode of action and metabolism of the drug while crossing the cell membrane and inside the cell. Despite the widespread use of cisplatin as an anticancer drug, there is still need for improvement [4] with respect to: (1) reduced toxicity; (2) increased clinical effectiveness;

*Email: aelsherif72@yahoo.com

Journal of Coordination Chemistry
ISSN 0095-8972 print/ISSN 1029-0389 online © 2011 Taylor & Francis
DOI: 10.1080/00958972.2011.587004

(3) broader spectrum of action; (4) elimination of side effects (e.g., nausea, hearing loss, vomiting, etc.); (5) increased solubility, and (6) ability to use them in combination with other drugs [5]. Replacement of the chloro ligands by carboxylates in carboplatin [6], cis-diamine (1,1-cyclobutanedicarboxylate) platinum(II), is a widely used second-generation platinum anticancer drug [7]; it does not cause the loss of high-frequency hearing or significant renal toxicity. Cisplatin and other second-generation platinum drugs have drawbacks such as high nephorotoxicity, low water solubility, and relative inactivity against gastrointestinal tumors [8]. Furthermore, the development of acquired resistance to cisplatin is frequently observed during chemotherapy [9]. On this basis, Gill [8] recently reported several palladium complexes with bidentate amine ligands which have shown anticancer activity comparable to, or greater than, cisplatin. Some investigators have suggested that carboplatin is merely a pro-drug for cisplatin [10], whereas others have postulated a ring-opening reaction [11] of carboplatin followed by reaction with guanosine-5′-monophosphate (5′-GMP) forming *cis*-[Pt$(NH_3)_2$(CBDCA-O)(5′-GMP)]. The ring-opening reaction with DNA constituent was investigated kinetically through studies of [Pd(amine)(CBDCA)] with inosine-5′-monophosphate [12]. Although the antitumor activity of *cisplatin* or carboplatin is ascribed to interactions between the complex and DNA [13–15], a large amount of the platinum reacts with other biomolecules, such as proteins and enzymes. In the blood, where the Pt drug is administered by injection or infusion, several molecules are available for kinetic and thermodynamic competition [14, 15]. Sulfur-containing molecules have a high affinity for platinum and could form very stable bonds. Moreover, the interaction of Pt complexes with sulfur-containing biomolecules has been associated with negative phenomena and some drawbacks remain in clinical use, such as nephorotoxicity, gastrointestinal toxicity, ototoxicity, neurotoxicity, and drug resistance [16–18]. Reactions with thiol (SH) group of protein side chains (e.g., in glutathione and metallothionine) are thought to trap and deactivate the drug before it reaches its cellular DNA target to form 1,2-intrastrand cross-links with guanine bases [19]. Glutathione (GSH), a tripeptide with a sequence γ-glutamylcysteinylglycine (γ-glu-CysH-Gly), is the most prevalent intracellular thiol with concentrations up to 10 mmol L^{-1} and the most abundant low-molecular weight peptide. GSH has been adapted through evolution to perform many diverse functions. For instance, GSH protects cells from the toxic effects of reactive oxygen compounds and functions in catalysis, metabolism, and transport. GSH participates in reactions involving the synthesis of proteins and nucleic acids and in those detoxifying free radicals and peroxides. Also, GSH serves as a storage and transport form of cysteine. GSH is synthesized intracellularly and exported from the cell [20–22]. At present, it is not clear how platinum(II) species reach DNA, because Pt(II) has a high affinity for sulfur donors compared with nitrogen donors such as those of DNA nucleotides. Pd(II) and Pt(II) amine complexes have the same structure, with a reactivity five orders of magnitude higher for Pd(II) complexes, but similar thermodynamic parameters. Coordination geometry and complex formation processes of palladium(II) are very similar to those of platinum(II). Thus, palladium(II) is frequently used to mimic the binding properties of various platinum(II) species and it acts as a good model for analogous Pt(II) complexes in solution. Much work has been performed on equilibrium studies of palladium(II) complexes with aliphatic amines [23–25], and it is of considerable interest to extend this work to other palladium complexes with aromatic heterocycles as 2-(aminomethyl)-benzimidazole (AMBI). The aromatic heterocycles act as σ-donors and can also function as fairly

effective π-acceptors. The π-accepting properties can be involved in π–π stacking with purine and pyrimidine bases, enhancing complex formation with DNA subunits, which is the principal target in chemotherapy of tumors and increases the effectiveness of the drug. Benzimidazole is of considerable chemical and biological interest, as its 5,6-dimethyl derivatives are present in vitamin B_{12} and related biomolecules. In conjunction with our research program [26–32] directed to study metal complexes of biological significance, it is necessary to study complex formation equilibria of $[Pd(AMBI)(H_2O)_2]^{2+}$ with sulfur- and nitrogen-donor biologically relevant ligands. The equilibrium of the displacement reaction of coordinated inosine, as a typical DNA constituent, by glutathione, as a typical thiol ligand, was investigated. Ring opening of chelated 1,1-cyclobutane dicarboxylic acid (CBDCA) and monodentate chelation of DNA constituents in the [Pd(AMBI)–CBDCA–DNA] system was studied. The effect of dioxane concentration on the formation of [Pd(AMBI)–CBDCA] (as a representative example) is also investigated. We also report the synthesis and characterization of palladium(II) complexes of 2-(aminomethyl)-benzimidazole and amino acids such as glycine, alanine, cysteine, serine, and methionine. The biological activity of the isolated complexes was screened.

2. Experimental

$PdCl_2$ and 2-(aminomethyl)-benzimidazole dihydrochloride hydrate (AMBI) were obtained from Aldrich Chem. Co. Glycine, alanine, lysine, thymine, uracil, uridine, aspartic acid, cysteine, glutathione (GSH), imidazole, inosine 5′-monophosphate, and threonine were provided by Sigma Chemical company and used without purification.

2.1. *Synthesis of [Pd(AMBI)(Cl$_2$)]*

In this study, $[Pd(AMBI)Cl_2]$ was prepared by heating $PdCl_2$ (532.2 mg, 3 mmol) in 50 mL water and KCl (447 mg, 6 mmol) to 50°C for 30 min. After the $K_2[PdCl_4]$ solution cooled, 2-(aminomethyl)-benzimidazole (660.2 mg, 3 mmol), dissolved in 10 mL water, was added dropwise with stirring. A yellow precipitate formed, and the mixture was stirred for a further 1 h at 25°C. After the precipitate was filtered off, it was washed sequentially with water, ethanol and diethyl ether. Yield (80%). Anal. Calcd for $C_8H_9N_3Cl_2Pd$: C, 29.6; H, 2.7; N, 12.9; and Cl, 21.8. Found: C, 30.0; H, 2.8; N, 13.0; and Cl, 21.5.

2.2. *Conversion of [Pd(AMBI)(Cl$_2$)] into the diaquo complex*

For equilibrium studies, $[Pd(AMBI)Cl_2]$ was converted into the diaquo complex $[Pd(AMBI)(H_2O)_2](NO_3)_2$ by stirring the chloro complex with two equivalents of $AgNO_3$ overnight and removing the AgCl precipitate by filtration through a 0.1 μm pore membrane filter. Great care was taken to insure that the resulting solution was free of Ag^+ and that the chloro complex had been converted into the aqua species; the filtrate was made up to the desired volume in a standard volumetric flask.

2.3. *Synthesis of palladium complexes*

2.3.1. [Pd(AMBI)(Gly)]Cl·H_2O (1). [Pd(AMBI)Cl_2] (337.42 mg, 1 mmol) was suspended in 50 mL of water at 60°C with glycine (75 mg, 1 mmol) and $NaHCO_3$ (84 mg, 1 mmol). The reaction mixture was stirred at 60°C for 4 h to a clear solution. The clear pale yellow solution was filtered and concentrated to 10 mL in a rotatory evaporator. The precipitate was filtered and washed with water, methanol, and diethyl ether. The compound was dried in vacuum at room temperature.

2.3.2. [Pd(AMBI)(Ala)]Cl·H_2O (2). [Pd(AMBI)Cl_2] (337.42 mg, 1 mmol) was suspended in 50 mL of water at 60°C with alanine (89 mg, 1 mmol) and $NaHCO_3$ (84 mg, 1 mmol). The reaction mixture was stirred at 50°C for 4 h to a clear solution. The clear pale yellow solution was filtered and concentrated to 10 mL in a rotatory evaporator. The orange–yellow precipitate was filtered and washed with water, methanol, and diethyl ether. The compound was dried in vacuum at room temperature.

2.3.3. [Pd(AMBI)(Cys)] (3). [Pd(AMBI)Cl_2] (337.42 mg, 1 mmol) was dissolved in 50 mL of ethanol and stirred with cysteine (121 mg, 1 mmol) and sodium bicarbonate (168 mg, 2 mmol) to a clear solution. The solution was filtered and concentrated to 10 mL at 50°C in a rotatory evaporator. The orange precipitate was filtered and washed with water, methanol, and diethyl ether. The compound was dried in vacuum at room temperature.

2.3.4. [Pd(AMBI)(Ser)]Cl·H_2O (4). [Pd(AMBI)Cl_2] (337.42 mg, 1 mmol) was dissolved in 50 mL of ethanol and stirred at room temperature with serine (105.09 mg, 1 mmol) dissolved in 1N NaOH (1 mL, 1 mmol) to a clear solution. This clear solution was concentrated to 3 mL in a rotatory evaporator at room temperature. The yellow precipitate was filtered and washed with water, methanol, and diethyl ether. The compound was dried in vacuum at room temperature.

2.3.5. Pd(AMBI)(Met)]Cl·H_2O (5). [Pd(AMBI)Cl_2] (337.42 mg, 1 mmol) was dissolved in 50 mL of ethanol and stirred at room temperature with serine (149 mg, 1 mmol) dissolved in 1N NaOH (1 mL, 1 mmol) to a clear solution. This clear solution was concentrated to 3 mL in a rotatory evaporator at room temperature. The yellow precipitate was filtered and washed with water, methanol, and diethyl ether. The compound was dried in vacuum at room temperature.

2.4. *Apparatus*

Potentiometric measurements were made using a Metrohm 686 titroprocessor equipped with a 665 Dosimat (Switzerland-Herisau). A thermostatted glass-cell equipped with a magnetic stirring system, a Metrohm glass electrode, a thermometric probe, a microburette delivery tube, and a salt bridge connected with the reference cell filled with 0.1 mol L^{-1} KCl solution in which saturated calomel electrode was dipped were used. The titroprocessor and electrode were calibrated daily with standard buffer solutions

prepared according to NBS specifications at $25.0 \pm 0.1^{\circ}C$ [33] and $I = 0.1\,mol\,dm^{-3}$, potassium hydrogen phthalate (pH 4.008), and a mixture of KH_2PO_4 and Na_2HPO_4 (pH 6.865). The microchemical analyses of the separated solid complexes for C, H, and N were performed in the Microanalytical Center, Cairo University. The analyses were performed twice to check the accuracy of the data. IR spectra were recorded on a Perkin Elmer FT-IR type 1650 spectrophotometer with KBr discs. The solid reflectance spectra were measured on a Shimadzu 3101 pc spectrophotometer. ^{1}H-NMR spectra were recorded using a Bruker ARX-300 spectrophotometer. Tetramethylsilane was used as internal standard and deuterated dimethyl sulfoxide (DMSO-d_6) as solvent. The molar conductance measurements of the Pd(II) complexes were determined in DMSO ($10^{-3}\,mol\,L^{-1}$) at room temperature using a Sybron-Barnstead conductometer.

2.5. *Procedure and measuring techniques*

The acid dissociation constants of the ligands were determined potentiometrically by titration ($1.25 \times 10^{-3}\,mol\,dm^{-3}$) of the ligand solution. The acid-dissociation constants of coordinated water in $[Pd(AMBI)(H_2O)_2)]^{2+}$ were determined by titration ($1.25 \times 10^{-3}\,mol\,dm^{-3}$) of the complex solution. The formation constants of the complexes were determined by titration ($1.25 \times 10^{-3}\,mol\,dm^{-3}$) of the $[Pd(AMBI)(H_2O)_2]^{2+}$ and ($1.25 \times 10^{-3}\,mol\,dm^{-3}$) of the ligands in concentration ratios 1 : 1. The titration solution mixtures had a volume of 40 mL. Temperature was maintained constant inside the cell at $(25.0 \pm 0.1)^{\circ}C$ by circulating thermostated water through the double-wall titration vessel with a slow and constant stream of N_2 over the test solutions. The pH meter readings were converted into hydrogen ion concentration by titrating a standard acid solution ($0.05\,mol\,dm^{-3}$) *versus* standard NaOH solution ($0.05\,mol\,dm^{-3}$) at 25°C. The pH is plotted against p[H]. The relationship pH–p[H] = 0.05 was observed. In this analysis, [OH^-] was calculated using a pK_w value of 13.921 [34]. The ionic strength was adjusted to $0.1\,mol\,dm^{-3}$ using $NaNO_3$. Equilibrium constants evaluated from the titration data (table 1) are defined by equations (1) and (2), where M, L, and H stand for $[Pd(AMBI)(H_2O)_2]^{2+}$, ligand, and proton, respectively.

$$pM + qL + rH \rightleftharpoons M_pL_qH_r \tag{1}$$

$$\beta_{\pi\theta\rho} = \frac{[M_pL_qH_r]}{[M]^p[L]^q[H]^r} \tag{2}$$

2.6. *Data processing*

Calculations were obtained from *ca.* 100 data points in each titration using the computer program MINIQUAD-75 [35]. The stoichiometry and stability constants of the complexes formed were determined by trying various composition models. The model selected gave the best statistical fit and was chemically consistent with the titration data without giving any systematic drifts in the magnitudes of various residuals, as described elsewhere [35]. The fitted model was tested by comparing the experimental titration data points and the theoretical curve calculated from the values

Table 1. Formation constants of $M_pL_qH_r$ species in aqueous solution at 25 ± 0.1°C and $I = 0.1$ mol dm^{-3} ($NaNO_3$).

System	p	q	r[a]	$\log \beta$[b]	S[c]
Pd(AMBI)-OH[d]	1	0	−1	−4.69(0.07)	8.2−7
	1	0	−2	−12.78(0.06)	
	2	0	−2	−6.34(0.09)	
Glycine[d]	0	1	1	9.60(0.01)	1.5E−7
	0	1	2	11.93(0.03)	
	1	1	0	9.71(0.05)	6.1E−7
Imidazole	0	1	1	7.04(0.01)	2.6E−9
	1	1	0	7.52(0.032)	
	1	2	0	13.57(0.04)	1.3E−7
Glutathione	0	1	1	9.26(0.01)	1.5E−7
	0	1	2	17.63(0.01)	
	0	1	3	20.85(0.03)	
	1	1	0	14.98(0.01)	5.2E−8
	1	1	1	18.82(0.02)	
	1	1	2	22.46(0.04)	
Aspartic acid	0	1	1	9.68(0.01)	2.2E−8
	0	1	2	13.40(0.01)	
	1	1	0	9.85(0.02)	1.8E−7
	1	1	1	13.16(0.04)	
Threonine	0	1	1	9.06(0.01)	7.9E−8
	0	1	2	11.03(0.02)	
	1	1	0	10.23(0.04)	1.8E−8
	1	1	−1	2.14(0.03)	
Lysine	0	1	1	10.51(0.01)	1.4E−8
	0	1	2	19.71(0.02)	
	0	1	3	21.99(0.02)	
	1	1	0	10.21(0.06)	2.0E−7
	1	1	1	18.68(0.09)	
Inosine[d]	0	1	1	8.43(0.01)	5.0E−9
	1	1	0	10.02(0.04)	3.3E−6
	1	1	1	12.06(0.09)	
	1	1	2	14.40(0.08)	

[a]p, q and r are the stoichiometric coefficients corresponding to $Pd(AMBI)^{2+}$, L and H^+, respectively.
[b]Standard deviations are given within parentheses.
[c]Sum of square of residuals.
[d]Taken from ref. [28]. The coefficient −1 refers to induced ionizable proton.

Table 2. Formation constants for mixed-ligand complexes of $[Pd(AMBI)(H_2O)_2]$ with cyclobutanedicarboxylic acid and some DNA units at 25°C and 0.1 mol L^{-1} ionic strength.

System	l	p	q	r[a]	$\log \beta$[b]	S[c]
Uracil	1	1	1	0	14.07(0.05)	7.1E−7
Uridine	1	1	1	0	13.97(0.01)	2.2E−6
Thymin	1	1	1	0	14.20(0.07)	1.1E−6
Inosine monophosphate	1	1	1	0	14.33(0.05)	1.7E−7
	1	1	1	1	20.50(0.07)	

[a]l, p, q, and r are the stoichiometric coefficients corresponding to $Pd(AMBI)^{2+}$, CBDCA, DNA subunits and H^+, respectively.
[b]Standard deviations are given within parentheses.
[c]Sum of square of residuals.

of the acid dissociation constant of the ligand and the formation constants of the corresponding complexes. The results are summarized in tables 1 and 2. The species distribution diagrams were obtained using the program SPECIES [36] under the experimental condition employed. All measurements were carried out in our laboratory at Cairo University.

2.7. *Biological activity*

2.7.1. Antibacterial activity. The antibacterial activities of metal complexes and the blank (DMSO solvent) were studied against *Staphylococcus pyogenes* as Gram-positive and *Escherichia coli* as Gram-negative. Each compound was dissolved in DMSO and solutions of 1, 2.5, and 5 mg mL^{-1} were prepared separately. Paper discs of Whatman filter paper (no. 42) of uniform diameter (2 cm) were sterilized in an autoclave. Paper discs soaked in the desired concentration of complex solutions were placed aseptically in Petri dishes containing nutrient agar media (agar 20 g + beef extract 3 g + peptone 5 g) seeded with *S. pyogenes* and *E. coli* bacteria, separately. The petri dishes were incubated at 37°C. The diameter of the zone of inhibition was measured after 24 h of incubation. The antibacterial activity of a common standard antibiotic Tavanic was also recorded maintaining the same protocol as above and at the same concentration and solvent. The antibacterial results of the compounds were compared with the standard and percentage activity index for the complexes was calculated using the formula given below

$$\%\ \text{Activity index} = \frac{\text{Zone of inhibition by test compound (diameter)}}{\text{Zone of inhibition by standard (diameter)}} \times 100$$

2.7.2. In vitro cytotoxicity. The Pd(II) complexes were screened for their cytotoxicity against colon carcinoma (HCT116) and larynx carcinoma (HEP2) cells using the protocol of SRB assay [37]. Cells were plated in a 96-multiwell plate (10^4 cells per well) for 24 h before treatment with the compounds to allow attachment of cells to the wall of plate. Different concentrations of the test compound were added to the cell monolayer. Triplicate wells were prepared for each individual dose and IC_{50} is the mean of three values. Monolayer cells were incubated for 48 h at 37°C in air with 5% CO_2. After 48 h, cells were fixed, washed, and stained with Sulfo-Rhodamine-B stain. Excess stain was washed with acetic acid and the attached stain recovered with tris-EDTA buffer. Color intensity was measured in an ELISA reader. The average drug concentration (μg cm^{-3}) for 50% inhibition of tumor cell-growth was determined by plotting the surviving fraction *versus* drug concentration for each tumor cell line.

3. Results and discussion

3.1. *Equilibrium studies*

The acid dissociation constants of the ligands determined under the experimental conditions (25 ± 0.1°C and $I = 0.1$ mol dm^{-3}) are used in the calculations of stability

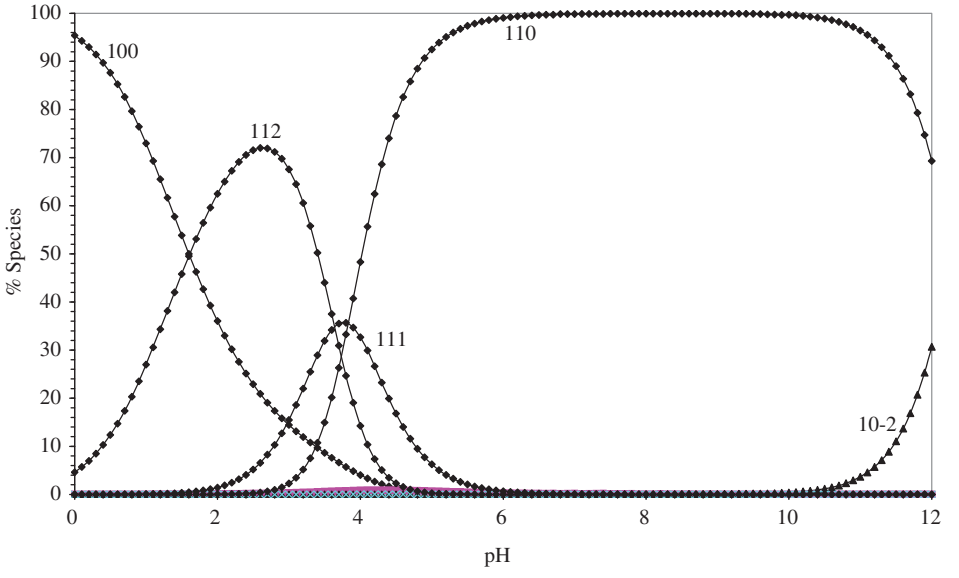

Figure 1. Concentration distribution as a function of pH in the Pd(AMBI)-glutathione system of 1.25×10^{-3} mol dm^{-3} for $Pd(AMBI)^{2+}$ and glutathione $I = 0.1$ mol dm^{-3} ($NaNO_3$) and $T = 25 \pm 0.1$°C.

constants of the Pd(II) complexes. The values obtained are consistent with data reported in the literature [38]. Analysis of the pH-titration data showed that the stability constant of $[Pd(AMBI)(H_2O)_2]^{2+}$ with amino acids is higher than for the corresponding monodentate imidazole (table 1). This indicates that the amino acids bind through amino and carboxylate groups.

3.1.1. Complex-formation equilibria of $[Pd(AMBI)(H_2O)_2]^{2+}$ with glutathione. Fitting the potentiometric data for the Pd(AMBI)-glutathione system indicated the formation of complex species with the stoichiometry coefficients 110, 111, and 112. Glutathione has various binding sites, namely oxygen of carboxylic group, nitrogen of amino group, and sulfur of sulfhydryl group. The stability constant of the (110) complex ($\log \beta = 14.98$) is higher than those of α-amino acids ($\log \beta_{[Pd(AMBI)(glycine)]} = 9.71$), indicating that glutathione interacts with Pd(II) by amino and deprotonated SH groups and not by the amino and caboxylate like simple α-amino acids. Also, this is in accordance with the fact that Pd(II) has a high affinity for S-donor ligands. The concentration distribution diagram given in figure 1 shows the formation of the protonated complex 112 with a formation degree of 72% at pH 2.6. By raising pH, the complex species (111) is formed with a concentration of 36% at pH 3.8. At pH 6, the complex species (110) predominates with a concentration of 99%, i.e., the reaction of $[Pd(AMBI)]^{2+}$ goes to completion in the physiological pH range. This may suggest that GSH will compete with DNA in reaction with the Pd(II) complex.

3.1.2. Complex-formation equilibria of $[Pd(AMBI)(H_2O)_2]^{2+}$ with threonine. Threonine has an extra binding center on the β-alcoholate group. This group was reported [39] to

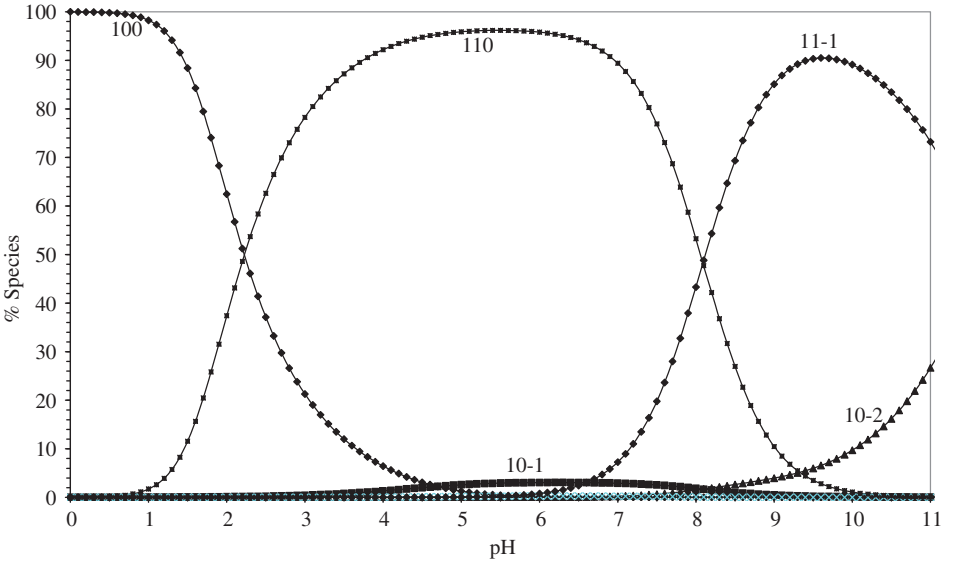

Figure 2. Concentration distribution as a function of pH in the Pd(AMBI)-threonine system of 1.25×10^{-3} mol dm^{-3} for Pd(AMBI)$^{2+}$ and threonine $I = 0.1$ mol dm^{-3} ($NaNO_3$) and $T = 25 \pm 0.1$°C.

participate in transition metal complex formation reactions. The potentiometric data are much better fitted assuming formation of 110 and 11−1. The pK_a value of the alcohol group incorporated in the Pd(II) complex ($\log \beta_{110}$–$\log \beta_{11-1}$) is 8.09; this is supported by the observation that in basic solutions, Cu(II) promotes ionization of the alcohol group of threonine with pK_a value of 10.3 [40]. The distribution diagram for the threonine complex is given in figure 2. The complex species with coefficients 110 reaches maximum degree of formation (95%) at pH 5–6, i.e., in the physiological pH range. However, the species 11−1 predominates after pH 9.5 and attains maximum concentration (90%) at pH 10.

3.1.3. Complex-formation equilibria of $[Pd(AMBI)(H_2O)_2]^{2+}$ with aspartic acid. Aspartic acid has two carboxylic and one amino group as potential chelating centers, coordinating either by two carboxylates or by the amino and one carboxylate. The stability constant of the aspartic acid complex is in the range of those for amino acids ($\log \beta_{[Pd(AMBI)(glycine)]} = 9.71$). This may reveal that aspartic acid coordinates by the amino and one carboxylate, leaving the extra carboxylate susceptible to protonation. The pK_a of the protonated species is calculated by equation (3)

$$pK^H = \log \beta_{111} - \log \beta_{110} \quad (3)$$

The pK_a of the protonated species of Pd(AMBI)-aspartic acid is 3.31, higher than that of the protonated amino group NH_3^+ (p$K_a = 9.68$) but close to that of the protonated carboxylate (p$K_a = 3.72$), suggesting that the proton in the protonated complex would be located mainly on the carboxylate. This value corresponds to a protonated carboxylate of aspartic acid considering the increase in acidity due to complex formation.

3.1.4. Displacement reaction of coordinated inosine. N-donor ligands such as DNA constituents have an affinity for $[Pd(AMBI)(H_2O)_2]^{2+}$, which may have important biological implications. However, the preference of Pd(II) to coordinate to S-donors was demonstrated as given in table 1. These results suggest that Pd(II)–N adducts can easily be converted into Pd–S adducts. Consequently, the equilibrium constant for such conversion is of biological significance. If we consider inosine as a typical DNA constituent (represented by HL) and glutathione as a typical thiol ligand (represented by H_3B), the equilibria involved in the complex formation and displacement reactions are

$$\begin{aligned} &HL \rightleftharpoons H^+ + L^- \\ &H_3B \rightleftharpoons 3H^+ + B^{3-} \\ &\underset{(100)}{[Pd(AMBI)]^{2+}} + L^- \rightleftharpoons \underset{110}{[Pd(AMBI)L]^+} \end{aligned} \tag{4a}$$

$$\beta_{110}^{[Pd(AMBI)L]+} = [Pd(AMBI)L]^+/[Pd(AMBI)]^{2+}\,[L] \tag{4b}$$

$$\underset{(100)}{[Pd(AMBI)]^{2+}} + B^{3-} \rightleftharpoons \underset{(110)}{[Pd(AMBI)B]^-} \tag{5a}$$

$$\beta_{110}^{[Pd(AMBI)B]-} = [Pd(AMBI)B]^-/[Pd(AMBI)]^{2+}\,[B^{3-}] \tag{5b}$$

$$[Pd(AMBI)L]^+ + B^{3-} \rightleftharpoons [Pd(AMBI)B]^- + L^- \tag{6}$$

The equilibrium constant for the displacement reaction given in equation (6) is

$$K_{eq} = [Pd(AMBI)B]^-[L^-]/[Pd(AMBI)L]^+[B^{3-}] \tag{7}$$

Substitution from equations (4b) and (5b) in equation (7) results in

$$K_{eq} = \beta_{110}^{[Pd(AMBI)B]-}/\beta_{110}^{[Pd(AMBI)L]+} \tag{8}$$

The $\log \beta_{110}$ values for $[Pd(AMBI)L]^+$ and $[Pd(AMBI)B]^-$ taken from table 1 are 10.02 and 14.98, respectively; substitution in equation (8) results in $\log K_{eq} = 4.96$. These values clearly indicate how sulfhydryl ligands such as glutathione are effective in displacing the DNA constituent, i.e., the main target in tumor chemotherapy.

3.1.5. Ring-opening of [Pd(AMBI)(CBDCA)] and formation of [Pd(AMBI)(CBDCA-O)(DNA)]. Potentiometric data for the system consisting of $[Pd(AMBI)(H_2O)_2]^{2+}$, CBDCA, and DNA constituents uracil, uridine, thymine, or IMP were fitted assuming different models. The accepted model for thymine is consistent with the formation of the 1 110 species. The accepted model for IMP consists of 1 110 and 1111 species. The pK_a of the protonated complex is 6.17 (table 2) for the IMP complex, probably due to the phosphate. The quaternary complex of IMP is more stable than those of pyrimidines. This may be explained on the premise that the cyclobutane ring forms a close hydrophobic contact with the purine ring of IMP. Such hydrophobic contacts may contribute to stabilization of the quaternary complexes. The same finding was obtained from a nuclear magnetic resonance (NMR) investigation of the ring-opening reaction of

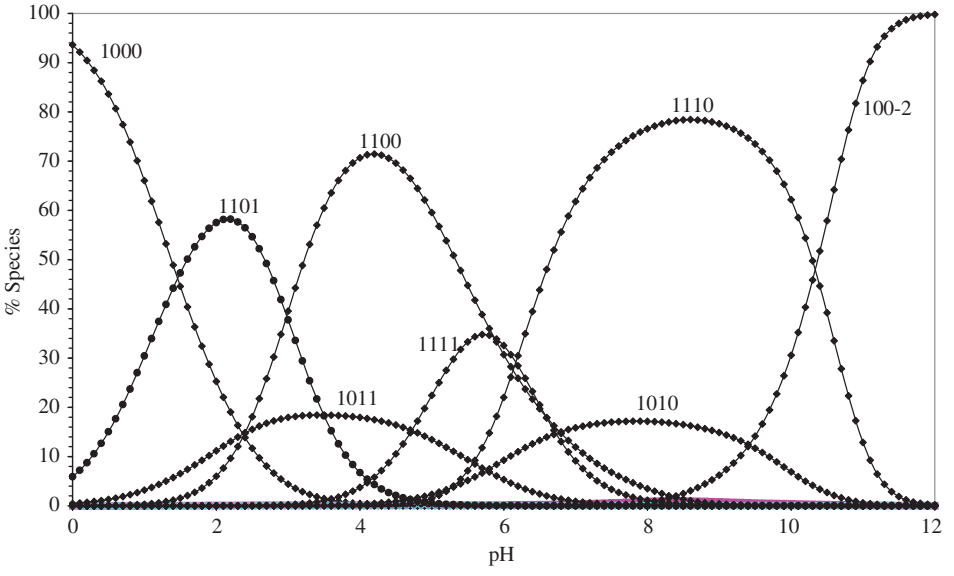

Figure 3. Concentration distribution as a function of pH in the Pd(AMBI)–CBDCA–inosine monophosphate of 1.25×10^{-3} mol dm^{-3} for Pd(AMBI)$^{2+}$, CBDCA and inosine monophosphate, $I = 0.1$ mol dm^{-3} ($NaNO_3$) and $T = 25 \pm 0.1$°C.

carboplatin with 5′-GMP [41]. These studies conclude that CBDCA is attached through one carboxylate oxygen and 5′-GMP through N_7 of the purine base. Further studies are necessary to elucidate the ring opening of chelated CBDCA by DNA constituents, especially multinuclear NMR measurements. Estimation of the concentration distribution of the various species in solution provides a useful picture of metal ion binding. To illustrate the main features observed in the species distribution plots in these systems, the speciation diagram obtained for the Pd(AMBI)–CBDCA–IMP system is shown in figure 3. The Pd(AMBI)–CBDCA species (1100) predominates with a formation degree of 71% at pH = 4.2. The Pd(AMBI)-IMP species (1010) reaches maximum concentration of 17% at pH = 7.6. The quaternary species Pd(AMBI)–CBDCA–IMP (1110) attains a maximum of 78% at pH 8.2–8.8. This reveals that in the physiological pH range, ring opening of chelated CBDCA by DNA is quite feasible.

3.1.6. Effect of solvent. Traditionally, water has been considered as the solvent that best represents biological conditions, although a lower polarity has been detected in some biochemical micro-environments such as active sites of enzymes and side chains in proteins [42–46]. It was suggested that these properties approximately correspond to those (or can be simulated by those) existing in water/dioxane mixtures. Consequently, a study of Pd(AMBI)–CBDCA complex formation, taken as a typical example, in dioxane–water solutions of different compositions could be of biological significance. In order to characterize the formation equilibria of Pd(AMBI)–CBDCA in dioxane–water solutions, all other equilibria involved, namely acid–base equilibria of CBDCA and $[Pd(AMBI)(H_2O)_2]^{2+}$, have to be studied in the same solutions. The equilibrium constants are reported in table 3. Hydrolysis of Pd(AMBI)$^{2+}$ in dioxane–water leads to formation of the mono- and dihydroxy species. The dihydroxo-bridged dimer was not

Table 3. Effect of dioxane on the formation constants of Pd(AMBI)–CBDCA at 25°C.

System	Dioxane (%)	p	q	r[a]	$\log\beta$[b]	S[c]
Pd(AMBI)–CBDCA	12.5	0	1	1	6.16(0.01)	1.4E−7
		0	1	2	9.58(0.02)	
		1	1	0	8.02(0.07)	4.8E−7
		1	0	−1	−4.79(0.01)	
		1	0	−2	−12.94(0.04)	1.8E−7
Pd(AMBI)–CBDCA	25	0	1	1	6.57(0.01)	2.5E−8
		0	1	2	10.38(0.02)	
		1	1	0	8.39(0.03)	3.8E−7
		1	0	−1	−5.07(0.05)	
		1	0	−2	−13.64(0.04)	1.2E−8
Pd(AMBI)–CBDCA	37.5	0	1	1	7.06(0.01)	2.4E−8
		0	1	2	11.28(0.01)	
		1	1	0	8.78(0.03)	4.6E−7
		1	0	−1	−5.17(0.01)	
		1	0	−2	−13.97(0.06)	3.8E−8
Pd(AMBI)–CBDCA	50	0	1	1	7.63(0.03)	2.2E−8
		0	1	2	12.31(0.03)	
		1	1	0	9.08(0.06)	1.3E−7
		1	0	−1	−5.34(0.03)	
		1	0	−2	−14.47(0.08)	5.4E−7
Pd(AMBI)–CBDCA	62.5	0	1	1	8.09(0.05)	1.03E−8
		0	1	2	13.07(0.05)	
		1	1	0	9.45(0.04)	2.5E−6
		1	0	−1	−5.42(0.01)	
		1	0	−2	−14.77(0.05)	9.2E−7

[a]p, q, and r are the stoichiometric coefficients corresponding to Pd(AMBI), CBDCA, and H^+, respectively.

detected. The pK_a values of CBDCA and those of the coordinated water in $[Pd(AMBI)(H_2O)_2]^{2+}$ increase linearly with increasing dioxane concentration. This may be correlated with the ability of a solvent of relatively low dielectric constant to increase the electrostatic attraction between the proton and ligand anion in case of CBDCA and that between a proton and the hydrolyzed form of Pd(II) species. The variation in stability constant of $[Pd(AMBI)(H_2O)_2]^{2+}$ with CBDCA as a function of solvent composition is shown in figure 4. The stability constant for Pd(AMBI)–CBDCA increases linearly with increasing dioxane concentration. This is explained in terms of complex formation involving oppositely charged ions as in the Pd(AMBI)–CBDCA complex, which is favored by the low dielectric constant of the medium, i.e., with increasing dioxane concentration. The results show that the CBDCA complex with $Pd(AMBI)^{2+}$ will be more favored in biological environments of lower dielectric constant.

3.2. *Characterization of the isolated solid complexes*

Palladium(II) complexes of 2-aminomethylbenzimidazole, $[Pd(AMBI)(AA)]^{n+}$, where $n = 0$ or 1 and AA is the anion of glycine, alanine, serine, methionine, and cysteine, have been prepared by interaction of $[Pd(AMBI)Cl_2]$ with an appropriate anion of the amino acid. The formulation of the synthesized Pd(II) complexes is based on the elemental analysis, molar conductance, IR and ^{1}H-NMR spectroscopy. The analytical data and conductivity values are given in table 4. The molar conductance of cysteine complexes is $2.1\,\Omega^{-1}\,cm^2\,mol^{-1}$, proving that this complex is a nonelectrolyte [47]. However, the

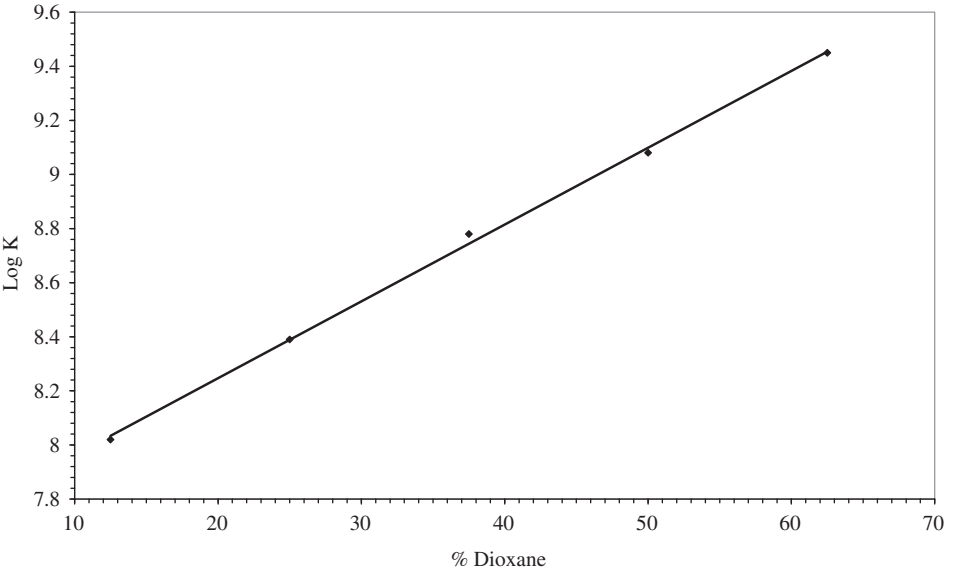

Figure 4. Effect of dioxane on the formation of the Pd(AMBI)–CBDCA system.

Table 4. Analytical data of complexes.

Complex	Molecular weight	Found (Calcd) (%)				
		C	H	N	Cl	S
[Pd(AMBI)(Gly)]Cl · $2H_2O$	398.92	30.12(30.08)	4.30(4.26)	14.10(14.03)	8.95(8.89)	–
[Pd(AMBI)(Ala)]Cl · H_2O	394.92	33.52(33.42)	4.33(4.30)	14.20(14.19)	9.02(8.99)	–
[Pd(AMBI)(Cys)]	372.42	35.53(35.44)	3.79(3.75)	15.07(15.03)	–	8.65(8.59)
[Pd(AMBI)(Ser)]Cl · H_2O	410.92	32.13(32.12)	4.15(4.13)	13.65(13.62)	8.70(8.64)	–
[Pd(AMBI)(Met)]Cl · H_2O	454.92	34.36(34.29)	4.63(4.61)	12.37(12.31)	7.83(7.80)	7.08(7.03)

other complexes show molar conductance values in the range 82–99, showing that they are 1 : 1 electrolytes [40]. Electronic absorption maxima of palladium(II) complexes are given in table 5. Bands at 322–328 nm are assigned to metal-to-ligand charge transfer (MLCT) from palladium to π-antibonding orbital of AMBI. Bands at 241–246 and 203–212 nm are due to n–π^* and π–π^* intraligand transitions, respectively [48].

In the absence of X-ray crystallography, IR spectra are the most suitable technique to elucidate bonding of the ligands to metal. The main IR bands with their tentative assignments are summarized in table 6. The infrared spectrum of the free ligand shows one medium and broad absorption in the region 3340–3280 cm^{-1} that are stretching vibrations of –NH and $–NH_3^+$. This band is shifted to lower frequencies in the Pd(II) complexes (3220–3000 cm^{-1}), showing that the amino group of AMBI coordinates to Pd(II). The free ligand shows one medium absorption band at 1630 cm^{-1} due to the stretch of (–C=N–) of the imidazole ring. In all the Pd(II) complexes, a medium band at 1580–1570 cm^{-1} can be attributed to υ(–C=N–) of the imidazole ring. The shift of 50–60 cm^{-1} of υ(–C=N) in the complexes indicates involvement of azomethine nitrogen in complexation [49, 50]. The strong band at 1248 cm^{-1}, due to the benzimidazole ring

Table 5. Electronic absorption spectra and conductance measurements of $[Pd(AMBI)(AA)]^{n+}$ complexes.

Complex	Λ_M[a]	λ_{max} (cm^{-1})		
		MLCT	n–π^*	π–π^*
$[Pd(AMBI)(Gly)]Cl \cdot 2H_2O$	85	325	246	212
$[Pd(AMBI)(Ala)]Cl \cdot H_2O$	82	327	245	210
[Pd(AMBI)(Cys)]	2.1	322	241	207
$[Pd(AMBI)(Ser)]Cl \cdot H_2O$	88	324	244	205
$[Pd(AMBI)(Met)]Cl \cdot H_2O$	99	328	243	203

[a]Molar conductance measured for 10^{-3} mol L^{-1} DMSO solution, Ω^{-1} cm^2 mol^{-1}.

Table 6. Tentative assignment of the important infrared bands of the synthesized ternary complexes.

Complex	Assigned wave numbers (cm^{-1})							
	υH_2O	υNH, NH_3^+	υC=N	υCOO^- (asymmetric)	υCOO^- (symmetric)	υPd–N	υPd–O	υPd–S
$[Pd(AMBI)(Gly)]Cl \cdot 2H_2O$	3485	3200–3000	1570	1605	1404	480	555	–
$[Pd(AMBI)(Ala)]Cl \cdot H_2O$	3496	3210–3090	1575	1610	1401	490	550	–
[Pd(AMBI)(Cys)]	–	3220–3100	1575	1648	–	495	–	385
$[Pd(AMBI)(Met)]Cl \cdot H_2O$	3490	3125–3040	1580	1645	–	488	–	390
$[Pd(AMBI)(Ser)]Cl \cdot H_2O$	3510	3138–3065	1572	1610	1395	492	545	–

in the free ligand, shifts to higher frequencies in all complexes with lower intensity, suggesting coordination of metal by the pyridine of the benzimidazole [49]. The infrared spectra of palladium(II) complexes of glycine, alanine, cysteine, serine, and methionine show a $\upsilon(COO^-)$ band between 1605 and 1610 cm^{-1}, suggesting that a $-COO^-$ of amino acid is coordinated to palladium(II) [51, 52], based on the fact that unionized and uncoordinated carboxylate stretching band occurs at 1750–1700 cm^{-1} whereas the ionized and coordinated COO^- stretching band appears at 1650–1590 cm^{-1} [51]. Bands found between 1404 and 1395 cm^{-1} are assigned to $\upsilon_s(COO^-)$. Deacon and Phillips [53] showed that the magnitude of $\Delta\nu$ [$\Delta\nu = \nu_{asy}(COO^-) - \nu_{sym}(COO^-)$] can be correlated with the coordination modes of carboxylate [54]. This difference is found to be > 200 cm^{-1}, reflecting monodentate coordination of carboxylate in the synthesized complexes. The infrared spectrum of free cysteine shows S–H stretch at 2568 cm^{-1}, which is absent in the cysteine complex. This suggests that the ionized and $-S^-$ of cysteine in its complex is coordinated to palladium(II) [55]. Also, cysteine complex shows a $\upsilon(COO^-)$ band at 1648 cm^{-1}, indicative of the presence of uncoordinated $-COO^-$. The υ(O–H) of free serine is unchanged under complex formation with $[Pd(AMBI)]^{2+}$, indicating that OH group does not participate in complex formation. Coordination of $-COO^-$ is confirmed by the presence of $\upsilon(COO^-)$ at 1610 cm^{-1} in the IR spectrum of the complex. The OH stretching frequency in spectra of Pd(II) complexes at 3500 cm^{-1} is attributed to the presence of water of hydration. Also, according to Stefov *et al.* [56], coordinated water exhibits frequencies at 825, 575, and 500 cm^{-1}. The absence of spectral bands in these regions indicates that water is not coordinated. Pd(II) complexes show bands at 545–555 cm^{-1} assigned to υ(Pd–O) of coordinated carboxylate while bands at 480–495 cm^{-1} are assigned to υ(Pd–N) [57].

Table 7. ^{1}H-NMR spectral data of $[Pd(AMBI)(AA)]^{n+}$ complexes.

Complex	Free AA		$[Pd(AMBI)(AA)]^{n+}$			
	δ_{Ha}	δ_{Hb}	δ_{Ha}	δ_{Hb}	δ_{-CH_2-} (AMBI)	$\delta_{\text{benzene ring-H}}$
$[Pd(AMBI)(Gly)]Cl \cdot 2H_2O$	3.59	–	3.88	–	3.7	7.4–7.1
$[Pd(AMBI)(Ala)]Cl \cdot H_2O$	3.79	1.49	4.05	1.62	3.6	7.3–7.0
[Pd(AMBI)(Cys)]	3.71	2.34	3.91	2.76	3.6	7.3–7.0
$[Pd(AMBI)(Met)]Cl \cdot H_2O$	3.49	2.08	3.68	2.50	3.5	7.4–7.1
$[Pd(AMBI)(Ser)]Cl \cdot H_2O$	4.05	4.05	4.14	4.09	3.6	7.3–6.9

^{1}H-NMR of the free AMBI · 2HCl: δ_{-CH_2-} (4.2) and $\delta_{\text{benzene ring-H}}$ (7.2–7.6 ppm).

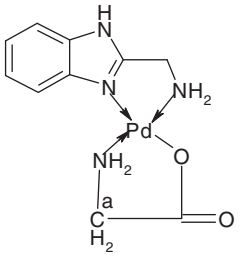

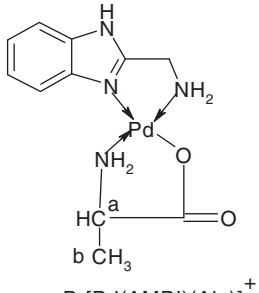

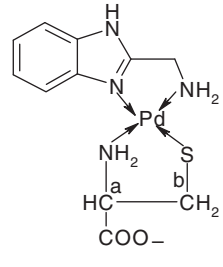

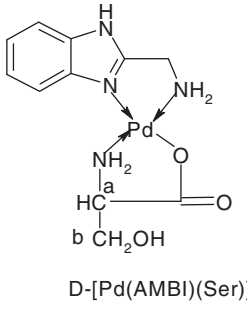

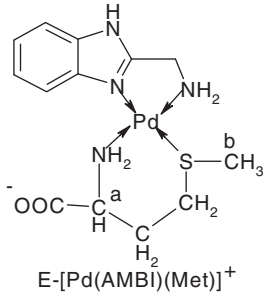

Figure 5. Structures (A)–(E) and numbering scheme of $[Pd(AMBI)(AA)]^{n+}$ complexes.

For Pd(II) complexes of l-cysteine and l-methionine, the Pd–S stretching vibrations are observed at 385 and 390 cm^{-1}, respectively [58].

The chemical shifts of the amino acid in the palladium(II) complexes are given in table 7. The structures of the palladium complexes along with the numbering scheme of protons are given in figure 5. The coordination of amino acids in their palladium complexes invariably produces downfield shift of their protons. The extent of downfield shift decreases regularly with distance from coordination site [59]. On coordination of $-NH_2$ and $-COO^-$ groups of amino acids, the proton attached to α-carbon becomes more deshielded than the corresponding amino acids in zwitterionic form because of donation of electron pairs to palladium by $-NH_2$ and $-COO^-$. The ^{1}H-NMR spectra of the free ligand (dihydrochloride salt) compared to the those of Pd(II) complexes show

considerable differences. The spectra of the complexes show upfield shift for the $-CH_2-$ of AMBI due to complexation. However, the $\delta(-CH_2-)$ of AMBI are invariably shifted upfield in the amino acid complexes compared to corresponding proton chemical shifts of $[Pd(AMBI)Cl_2]$ ($\delta-CH_2- = 3.9$). This can be attributed to stronger binding of amino acids than chloride to palladium(II) [60]. Thus, the ^{1}H-NMR spectra show that Pd(II) is bound to $-NH_2$ of the side chain of the benzimidazole ring and the pyridine type nitrogen of the benzimidazole in these complexes.

The ^{1}H-NMR spectrum of $[Pd(AMBI)(Gly)]Cl \cdot 2H_2O$ shows a singlet at 3.88 ppm corresponding to two protons of coordinated glycine. The corresponding proton of glycine in zwitterionic form resonates at 3.59 ppm. The downfield shift of 0.29 ppm suggests binding of N of the ($-NH_2$) group and (O) of the carboxylate group of glycine to palladium(II). The $\upsilon(COO^-)$ band in the IR spectrum of the complex at 1605 cm^{-1} suggests further that the $-COO^-$ group is coordinated to palladium(II). Thus, the complex structure of [Pd(AMBI)(Gly)] has been assigned, as shown in figure 5(A).

The ^{1}H-NMR spectrum of alanine in the zwitterionic form gives a quartet due to H_a and doublet due to H_b at 3.79 and 1.49 ppm, respectively (table 7). The corresponding protons of $[Pd(AMBI)(Ala)]Cl \cdot 2H_2O$ appear at 4.05 and 1.62 ppm, respectively. The larger downfield shift of 0.26 ppm of H_a confirms coordination of N– of $-NH_2$ and O of COO^- to palladium(II). The $\upsilon(COO^-)$ at 1610 cm^{-1} in the complex suggests the structure (B) as given in figure 5(B).

The ^{1}H-NMR spectrum of the cysteine complex gives a triplet due to H_a and doublet due to H_b at 3.92 and 2.76 ppm, respectively (table 7). The corresponding protons of free cysteine appear at 3.71 and 2.34 ppm, respectively. Similar shifts have been observed in the corresponding platinum(II) complex [57]. Thus, the ^{1}H-NMR spectrum of cysteine complex supports the binding of cysteine to palladium through N of $-NH_2$ and S^- of deprotonated –SH shown in figure 5(C).

The ^{1}H-NMR spectrum of $[Pd(AMBI)(Ser)]Cl \cdot H_2O$ shows a downfield shift of H_a, confirming the binding of nitrogen of $-NH_2$ and oxygen of $-COO^-$ of serine to palladium(II). The $\upsilon(COO^-)$ at 1395 cm^{-1} in IR spectrum of this complex is further indicative of the binding of $-COO^-$ of serine to palladium(II). Thus, the complex structure has been assigned as shown in figure 5(D), also in accord with its molar conductance as a 1 : 1 electrolyte.

The ^{1}H-NMR spectrum of methionine complex shows a downfield shift of 0.42 ppm in H_b compared to the corresponding proton of free methionine (table 7). This suggests that sulfur of $-S-CH_3$ of methionine is coordinated to palladium. The H_a proton (attached to the α-carbon) of methionine moiety in the complex experiences a downfield shift of 0.19 ppm compared to the corresponding proton of free methionine. This can be interpreted by the coordination of nitrogen of $-NH_2$ and oxygen of $-COO^-$ to palladium. This, together with $\upsilon(COO^-)$ at 1645 cm^{-1} in the complex and 1 : 1 electrolyte, supports the structure given in figure 5(E).

3.3. *Antibacterial activity*

Bacteria can achieve resistance to antibiotics through biochemical and morphological modifications [61]. Therefore, finding new compounds with antibacterial activity is of paramount importance and of interest to assess the biological potential of the synthesized Pd(II) complexes. Antibacterial activities were performed against one

Table 8. Antibacterial activity of Pd(II)-complexes.

Compounds	*S. pyogenes* (Gram-positive)						*E. coli* (Gram-negative)					
	Diameter of inhibition zone (mm)			Activity index (%)			Diameter of inhibition zone (mm)			Activity index (%)		
Concentration ($mg\,mL^{-1}$)	1.0	2.5	5.0	1.0	2.5	5.0	1.0	2.5	5.0	1.0	2.5	5.0
$[Pd(AMBI)(Gly)]Cl \cdot 2H_2O$	2	5	10	50	56	71	3	7	11	60	70	73
$[Pd(AMBI)(Ala)]Cl \cdot H_2O$	2	6	11	50	67	79	3	7	12	60	70	80
[Pd(AMBI)(Cys)]	3	9	13	75	89	93	4	9	14	80	90	94
$[Pd(AMBI)(Met)]Cl \cdot H_2O$	4	9	13	75	89	93	4	9	15	80	90	100
$[Pd(AMBI)(Ser)]Cl \cdot H_2O$	3	7	12	75	78	86	3	8	13	60	80	87
Tavanic (standard)	4	9	14	100	100	100	5	10	15	100	100	100

Gram-positive (*S. pyogenes*) and another Gram-negative (*E. coli*) bacteria at different concentrations 1, 2.5, and $5\,mg\,mL^{-1}$ in DMSO using Tavanic as standard material. The diffusion agar technique was used for screening antibacterial activity of the synthesized complexes [62–65]. The medium used for growing the culture was nutrient agar. The results of the bactericidal screening of the synthesized compounds are recorded in table 8. The results show that activity of the complexes against *E. coli* is better than against *S. pyogenes*. It is observed that [Pd(AMBI)(Met)] and [Pd(AMBI)(Cys)] have higher antibacterial activities than the other complexes. Activity of these compounds against *S. pyogenes* decreased in the order Tavanic > [Pd(AMBI)(Met)] ~ [Pd(AMBI)(Cys)] > [Pd(AMBI)(Ser)] > [Pd(AMBI)(Ala)] > [Pd(AMBI)(Gly)] and against *E. coli* decreased in the order Tavanic ~ [Pd(AMBI)(Met)] > [Pd(AMBI)(Cys)] > [Pd(AMBI)(Ser)] > [Pd(AMBI)(Ala)] > [Pd(AMBI)(Gly)] under experimental conditions. Activity of the complexes increases as the concentration increases [66, 67]. Antibacterial activity of all mixed ligand complexes toward *E. coli* indicates that these complexes could be applied in the treatment of some common diseases caused by *E. coli*, e.g., septicemia, gastroenteritis, urinary tract infections, and hospital-acquired infections [68, 69].

3.4. *Cytotoxic activities*

Cytotoxic study of the compounds against colon carcinoma (HCT116) and larynx carcinoma (HEP2) cells indicate that $[Pd(AMBI)(Met)]Cl \cdot H_2O$ shows significant activity against (HCT116) cells with IC_{50} value $0.74\,\mu g\,mL^{-1}$, while [Pd(AMBI)(Cys)] shows activity against (HEP2) with IC_{50} value $0.60\,\mu g\,mL^{-1}$ (figure 6), classifying these compounds as chemotherapeutically significant (table 9). It was suggested that S,N-chelate complexes of Pd(II) were expected to exhibit more anti-tumor and anti-microbial activities [70, 71]. IC_{50} is the concentration which can reduce the growth of cancer cells by 50%. Results show that the growth inhibition of tumor cells is due to apoptosis (programmed cell death) in all Pd(II) complexes. Induction of apoptosis was thought to be one of the mechanisms of the antitumor effect of cisplatin [72]. The new compounds reported here show less nephrotoxicity because the tightly bound amino acid ligands may be difficult to replace *in vivo* by the protein-bound sulfhydryl groups of the kidney tubule cells. The high chloride concentration of the gastrointestinal region

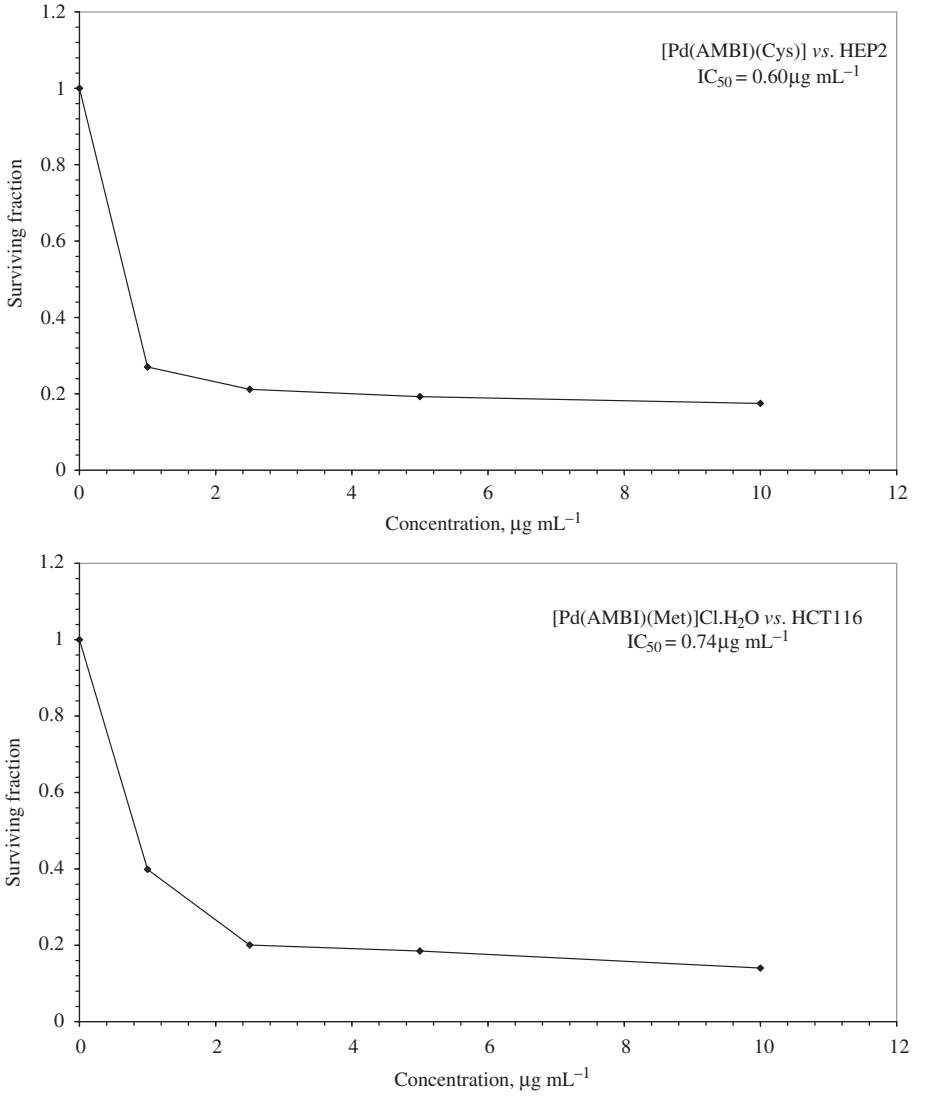

Figure 6. Effect of [Pd(AMBI)(Cys)] and [Pd(AMBI)(Met)] complexes on surviving fraction of HEP2 and HCT116 tumor cells, respectively.

is responsible for the failure of cisplatin in the treatment of tumors of this region [73]. The palladium complexes reported here are not expected to interact further with chloride, and therefore are expected to be useful for the treatment of tumors of the gastrointestinal region.

4. Conclusions

This investigation describes complex formation equilibria of a $[Pd(AMBI)(H_2O)_2]^{2+}$ with sulfur- and nitrogen-donor biologically relevant ligands. The equilibrium constants

Table 9. Effect of Pd(II)-complexes on tumor cell growth *in vitro* (IC_{50} values in $\mu g\,mL^{-1}$).

	IC_{50}	
Compounds	*HCT116*	HEP2
[Pd(AMBI)(Gly)]Cl · $2H_2O$	1.89	0.94
[Pd(AMBI)(Ala)]Cl · H_2O	1.72	0.82
[Pd(AMBI)(Cys)]	2.82	0.60
[Pd(AMBI)(Met)]Cl · H_2O	0.74	0.87
[Pd(AMBI)(Ser)]Cl · H_2O	1.54	0.74
Doxorubicin (standard)	0.69	0.40

IC_{50} = cytotoxic dose at 50%, i.e., the drug concentration to reduce the growth of the cancer cells by 50%.

were determined and speciation diagrams evaluated. The results show that the stability constant of $[Pd(AMBI)(H_2O)_2]^{2+}$ with amino acids is higher than for the corresponding monodentate imidazole, indicating that the amino acids bind through the amino and carboxylate groups. The extra carboxylate in aspartic acid does not contribute to the stability of the formed complex as the additional carboxylate does not compete with the amino group during complex formation. The β-alcoholate group in the side chain of the amino acid threonine plays an essential role in the functioning of a number of proteolytic enzymes, e.g., chymotrypsin and subtilisin. It is seen that $[Pd(AMBI)(H_2O)_2]^{2+}$ promotes ionization of the alcohol group of threonine. The pK_a of the alcohol incorporated in Pd(II) complex is 8.09, which indicates that participation of OH in complex formation is not contributing significantly in the physiological pH range. Reaction of $[Pd(AMBI)(H_2O)_2]^{2+}$ with glutathione is more favorable than α-amino acids, because GSH interacts with Pd(II) by amino and deprotonated SH groups. The formed complex increases with increasing pH, making complex formation more favorable in the physiological pH range, whereas at levels higher than physiological pH range, hydroxo species dominate. The equilibrium constant of the displacement reaction of coordinated inosine, as a typical DNA constituent, by glutathione, as a typical thiol ligand indicate how sulfhydryl ligands such as glutathione are effective in displacing the DNA constituent, i.e., the main target in tumor chemotherapy. Pd(AMBI)–CBDCA complex-formation equilibria in dioxane–water solutions of different compositions show that formation of Pd(AMBI)–CBDCA will be more favored in biological environments of lower dielectric constant. The prepared complexes show concentration-dependent antibacterial activity. It is seen that [Pd(AMBI)(Met)]Cl · H_2O and [Pd(AMBI)(Cys)] show significant activity against colon carcinoma (HCT116) and larynx carcinoma (HEP2) tumor cells. The palladium complexes reported here are expected to be useful for the treatment of tumors of the gastrointestinal region because the tightly bound amino acid ligands may be difficult to replace *in vivo* by protein-bound sulfhydryl groups of the kidney tubule cells.

References

[1] B. Rosenberg, L. Van Camp, J.E. Trasko, V.H. Mansour. *Nature*, **222**, 385 (1969).
[2] E. Wong, C.M. Giandomenico. *Chem. Rev.*, **99**, 2451 (1999).

[3] Z. Guo, P.J. Sadler. *Adv. Inorg. Chem.*, **49**, 183 (2000).
[4] J. Burchenal, K. Kalaher, K. Died, L. Lokys. *Cancer Treat. Res.*, **63**, 1493 (1979).
[5] J.B. Vermorken, H.M. Pinedo. *Neth. J. Med.*, **25**, 270 (1982).
[6] J.J. Roberts, R.J. Knox, F. Friedlos, D.A. Lydall. In *Biochemical Mechanisms of Platinum Anticancer Drugs*, D.C.H. Mc Brien, T.F. Slater (Eds), pp. 29–64, IRL Press, Oxford (1986).
[7] K.J. Barnham, M.I. Djuran, P.D.S. Murdoch, J.O. Ranford, P.J. Sadler. *Inorg. Chem.*, **35**, 1065 (1996).
[8] D.S. Gill. In *Platinum Coordination Complexes in Cancer Chemotherapy*, M.P. Hacker, E.B. Douple, I.H. Krakoff (Eds), pp. 267–278, Nijhoff, Boston (1984).
[9] M.E. Heim. In *Metal Complexes in Cancer Chemotherapy*, B.K. Keppler (Ed.), p. 9, VCH, Weinheim (1993).
[10] S.J. Berners-Price, P.W. Kuchel. *J. Inorg. Biochem.*, **38**, 327 (1990).
[11] L. Canovese, L. Cattalini, G. Chessa, M.L. Tobe. *J. Chem. Soc., Dalton Trans.*, 2135 (1988).
[12] A. Shoukry, T. Rau, M. Shoukry, R. Van Eldik. *J. Chem. Soc., Dalton Trans.*, 3105 (1998).
[13] E. Wong, C.M. Giandomenico. *Chem. Rev.*, **99**, 2451 (1999).
[14] J. Reedijk. *Chem. Rev.*, **99**, 2499 (1999).
[15] E.R. Jamieson, S.J. Lippard. *Chem. Rev.*, **99**, 2467 (1999).
[16] M.A. Fuertes, C. Alonso, J.M. Pérez. *Chem. Rev.*, **103**, 645 (2003).
[17] R.T. Door. In *Platinum and Other Metal Coordination Compounds in Cancer Chemotherapy*, H.M. Pinedo, J.H. Schornagel (Eds), pp. 131–154, Plenum, New York (1996).
[18] C.J. Ziegler, A.P. Silverman, S.J. Lippard. *J. Biol. Inorg. Chem.*, **5**, 774 (2000).
[19] P.M. Takahara, C.A. Frederic, S.J. Lippard. *J. Am. Chem. Soc.*, **1188**, 12309 (1996).
[20] P.C. Jocelyn. *Biochemistry of the SH Group*, p. 94, Academic Press, New York (1972).
[21] M. Friedman. *The Chemistry and Biochemistry of the Sulfhydryl Group in Amino Acids, Peptides and Proteins*, pp. 52–87, Pergamon, New York (1973).
[22] A.E. Clausen, C.E. Kast, A. Bernkop-Schnürch. *Pharm. Res.*, **19**, 602 (2002).
[23] M.M.A. Mohamed, M.M. Shoukry. *Polyhedron*, **20**, 343 (2001).
[24] M.M. Shoukry, M.R. Shehata, A. Abdel Razik, A.T. Abdel-Karim. *Mont. Fur. Chem.*, **130**, 409 (1998).
[25] S.M. El-Medani, S.M. Shohayeb, M.M. Shoukry. *Transition Met. Chem.*, **23**, 287 (1998).
[26] A.A. El-Sherif. *Inorg. Chim. Acta*, **362**, 4991 (2009).
[27] A.A. El-Sherif, M.M. Shoukry. *J. Main Group Met. Chem.*, **29**, 189 (2006).
[28] A.A. El-Sherif. *J. Solution Chem.*, **35**, 1287 (2006).
[29] N.A. Al-Awadi, N.M. Shuaib, A.A. El-Sherif, A. El-Dissouky, E. Al-Saleh. *Bioinorg. Chem. Appl.*, **2008**, Art. ID 479897 (2008).
[30] A.A. El-Sherif. *J. Solution Chem.*, **39**, 1562 (2010).
[31] M.M.A. Mahmoud, A.A. El-Sherif. *J. Solution Chem.*, **39**, 639 (2010).
[32] A.A. El-Sherif. *J. Solution Chem.*, **39**, 131 (2010).
[33] R.G. Bates. *Determination of pH-Theory and Practice*, 2nd Edn, Wiley-Interscience, New York (1975).
[34] A.A. El-Sherif. *J. Coord. Chem.*, **64**, 1240 (2011).
[35] P. Gans, A. Sabatini, A. Vacca. *Inorg. Chim. Acta*, **18**, 237 (1976).
[36] L. Pettit. University of Leeds, Personal Communication.
[37] P. Skehan, R. Storeng, D. Scudiero, A. Monks, J. McMahon, D. Vistica, J.T. Warren, H. Bokesch, S. Kenney, M.R. Boyd. *J. Natl. Cancer Inst.*, **82**, 1107 (1990).
[38] D.D. Perrin. *Stability Constants of Metal-Ion Complexes: Part B Organic Ligands*, Pergamon Press, Oxford (1979).
[39] M.C. Lim. *Inorg. Chem.*, **20**, 1377 (1981).
[40] P. Grenouillet, R.P. Martin, A. Rossi, M. Ptak. *Biochim. Biophys. Acta*, **322**, 185 (1973).
[41] U. Frey, J.D. Ranford, P.J. Sadler. *Inorg. Chem.*, **32**, 1333 (1993).
[42] D.O. Rees. *J. Mol. Biol.*, **141**, 323 (1980).
[43] N.K. Rogers, G.R. Roore, M.J.E. Strenberg. *J. Mol. Biol.*, **182**, 613 (1985).
[44] H. Sigel, R.B. Martin, R. Tribolet, U.K. Haring, R. Malini-Balakrishran. *Eur. J. Biochem.*, **152**, 187 (1985).
[45] G. Akerlof, O.A. Short. *J. Am. Chem. Soc.*, **75**, 6357 (1953).
[46] H. Sigel. *Pure Appl. Chem.*, **61**, 923 (1989).
[47] R.J. Angelici. *Synthesis and Technique in Inorganic Chemistry*, pp. 17–18, Saunders, Philadelphia, PA (1969).
[48] P.M. Gidney, R.D. Gillard, B.T. Heaton. *J. Chem. Soc., Dalton Trans.*, 2133 (1974).
[49] A. García-Raso, J.J. Fiol, B. Adrover, E. Molins, C. Miravitlles. *Polyhedron*, **15**, 1829 (1996).
[50] N. Bharti, M.R. Maurya, F. Nagvi, A. Azam. *Bioorg. Med. Chem. Lett.*, **10**, 2243 (2000).
[51] J.A. Kieft, K. Nakamoto. *J. Inorg. Nucl. Chem.*, **29**, 2561 (1967).
[52] K. Nakamoto. *Infrared and Raman Spectra of Inorganic and Coordination Compounds*, 3rd Edn, p. 311, Wiley, New York (1978).
[53] G.B. Deacon, R.J. Phillips. *Coord. Chem. Rev.*, **33**, 227 (1980).
[54] R.C. Mehrotra, R. Bohra. *Metal Carboxylates*, p. 48, Academic Press, New York (1983).
[55] H. Shindo, T.L. Brown. *J. Am. Chem. Soc.*, **87**, 1904 (1965).

[56] V. Stefov, V.M. Petrusevski, B. Soptrajanov. *J. Mol. Struct*., **293**, 97 (1993).
[57] M. Biddau, G. Devoto, M. Massacesi, G. Ponticelli. *Transition Met. Chem*., **1**, 99 (1976).
[58] G. Pneumatikakis, N. Hadjiliadis. *J. Inorg. Nucl. Chem*., **4**, 29 (1979).
[59] L.E. Erickson, J.W. McDonald, J.K. Howie, R.P. Clow. *J. Am. Chem. Soc*., **90**, 6371 (1968).
[60] L. Kumar, N.R. Kandasamy, T.S. Srivastava, A.J. Amonkar, M.K. Adwankar, M.P. Chitnis. *J. Inorg. Biochem*., **23**, 1 (1985).
[61] N. Sari, S. Arslan, E. Logoglu, I. Sakiyan. *J. Sci*., **16**, 283 (2003).
[62] M. Belicchi Ferrari, S. Capacchi, G. Pelosi, G. Reffo, P. Tarasconi, R. Albertini, S. Pinelli, P. Lunghi. *Inorg. Chim. Acta*, **286**, 134 (1999).
[63] C. Jayabalakrishnan, K. Natarjan. *Synth. React. Inorg. Met.-Org. Chem*., **31**, 983 (2001).
[64] T. Jeeworth, H.L.K. Wah, M.G. Bhowon, D. Ghoorhoo, K. Babooram. *Synth. React. Inorg. Met.-Org. Chem*., **30**, 1023 (2002).
[65] N. Dharmaraj, P. Viswanathamurthi, K. Natarajan. *Transition Met. Chem*., **26**, 105 (2001).
[66] R. Chaudhary, R.V. Singh. *Phosphorus, Sulfur, Silicon*, **178**, 603 (2003).
[67] A.A. El-Sherif, B.J.A. Jeragh. *Spectrochim. Acta, Part A*, **68**, 877 (2007).
[68] D.C. Shanson. *Microbiology in Clinical Practice*, Wright PSG, Bristol, London, Boston (1982).
[69] E. Jawetz, J.L. Melnick, E.A. Adelberg. *Review of Medical Microbiology*, 6th Edn, Lang Medical Publications, Los Angeles, CA (1979).
[70] M. Das, S.E. Livingstone. *Br. J. Cancer*, **37**, 466 (1978).
[71] A. Garoufis, S.K. Hadjikakou, N. Hadjiliadis. *Coord. Chem. Rev*., **253**, 1384 (2009).
[72] M.A. Barry, C.A. Behnke, A. Eastman. *Biochem. Pharmacol*., **40**, 2353 (1990).
[73] M.J. Cleare, P.C. Hyde. In *Metal Ions in Biological Systems*, H. Sigel (Ed.), Vol. 11, p. 1, Marcel Dekker, New York (1980).